Chapter 7

Conclusion

7.1 Summary of the Thesis

7.1.1 Development of the Optoelectronic SFL

We have demonstrated the use of optoelectronic feedback for precise control over the optical chirp of a semiconductor laser diode. This system, the optoelectronic SFL, formed the backbone of all the work described in this thesis. The development of the optoelectronic SFL was guided by optical FMCW reflectometry and 3-D imaging applications. Specifically, we aimed to build a swept-source with narrow linewidth (for long-range imaging), linear frequency tuning (to reduce the processing overhead), and high chirp bandwidth (for high axial resolution), all on a compact platform without moving parts.

The optoelectronic SFL works like a PLL. A portion of the SCL light is launched into a Mach-Zehnder interferometer, and the loop locks the sinusoidal intensity fluctuation at the interferometer output to a reference electronic oscillator. The optoelectronic SFL, just as a regular PLL, only achieves lock if the feedback bandwidth is larger than the unlocked beat signal linewidth, which is determined by the free-running SCL chirp nonlinearity. As the SCL is chirped faster, the nonlinearity is increased, which lead to poor locking—our initial experiments were limited to a chirp rate of 10^{14} Hz/s for DFB lasers and 5×10^{14} for VCSELs. To improve the free-running sweep nonlinearity, we developed a bias current predistortion algorithm. Even though the algorithm was based on a very naive nonlinear tuning model, it yielded impressive results when iterated. Using iterative predistortion we were able to significantly increase the chirp rates of our systems, up to 10^{15} Hz/s for DFB lasers and 10^{16} for VCSELs. We developed SFLs based on VCSELs and DFB lasers at wavelengths of 1550 nm and 1060 nm, and demonstrated their use in reflectometry and profilometry applications. Electronic development of the SFL undertaken as part of our work eventually lead to its commercialization by Telaris, Inc.

A key feature of the optoelectronic SFL, albeit not one that we recognized until after the first system was built and tested, is that successive chirps are exactly repeatable. The PLL locks not just the beat signal frequency, i.e., the instantaneous chirp rate, but also the beat signal phase, i.e., the starting chirp frequency. This means that each frequency sweep starts at the exact same point. As it turned out, stability of the starting sweep frequency was crucial for our work on MS-FMCW reflectometry and TomICam.

7.1.2 Ranging and 3-D Imaging Applications

7.1.2.1 MS-FMCW Reflectometry and Stitching

In an effort to increase the axial resolution of an SCL-based ranging system, we developed a novel variant of the FMCW optical imaging technique. This method, MS-FMCW reflectometry, uses multiple lasers that sweep over distinct but adjacent regions of the optical spectrum, in order to "stitch" a measurement with increased optical bandwidth and a corresponding improvement in the axial resolution. This technique bears resemblance to synthetic aperture radar, in which RF signals collected at multiple physical locations are used to approximate a large antenna aperture, and hence a high transverse resolution. In MS-FMCW reflectometry, the synthesized aperture is not physical, but instead represents the accessible optical frequency range.

The culmination of this work was an MS-FMCW system with four VCSEL channels, yielding a total chirp bandwidth of 2 THz and a scan time of 500 μs. This particular demonstration relied on hardware stitching to remove the need for additional signal processing that was present in our early MS-FMCW work. In a hardware stitching system, the SCL sweeps are locked to the same MZI with an electronic reference oscillator whose phase is not reset during channel switching. Because the starting frequencies of the sweeps are controlled exclusively by the reference oscillator phase, this configuration allowed perfect stitching to be performed in hardware. Each channel's chirp started precisely where the previous one ended!

7.1.2.2 The Tomographic Imaging Camera

One of the goals of our work is to enable rapid, high-resolution, and low-cost 3-D imaging without moving parts. The tomographic imaging camera was our solution to the problem of non-mechanical acquisition of transverse pixel information. TomICam uses low-cost full-field detector arrays to acquire depth information one transverse slice at a time. This is achieved by modulating the intensity of the transmitted beam with sinusoidal function, which shifts the signal spectrum to DC, allowing the use of low-speed integrating detector arrays, i.e., CCD and CMOS cameras. The depth of the slice is determined by the modulation frequency, and can therefore be tuned electronically. As a result, TomICam completely eliminates the need for moving parts traditionally employed in 3-D imaging.

We demonstrated basic TomICam functionality in a single-pixel proof-of-concept experiment at 1550 nm, and showed that the depth scan retrieved with TomICam is identical to the traditional FMCW measurement. It turns out that multiple measurements (two to four, depending on whether or not the imaging interferometer is balanced) at the same modulation frequency but different modulation phases are necessary to extract the depth information. This means that TomICam imaging would not be possible if there was appreciable starting frequency jitter between subsequent SFL sweeps. For TomICam, as for MS-FMCW, precise repeatability of the frequency sweeps generated by the optoelectronic SFL turned out to be a necessary requirement. We also discussed the application of compressive sensing to the TomICam platform, and showed, through computer simulations, that a tenfold improvement in the volume acquisition speed is possible for sufficiently sparse depth signals.

7.1.3 Phase-Locking and CBC of Chirped Optical Waves

Out group's current focus on the phase and frequency control of SCLs started a few years ago with phase-locking and coherent beam combining experiments that used commercially available, single-frequency semiconductor laser diodes. We have generalized these experiments to the case of chirped optical waves. The precise chirp linearity of the optoelectronic SFL enables non-mechanical compensation of optical delays using acousto-optic frequency shifters, and is at the heart of our chirped phase-locking and coherent-combining systems.

We have demonstrated heterodyne phase-locking of optical waves with a chirp rate of 5×10^{14} Hz/sec at 1550 nm, and constructed a dual-channel passive-fiber coherent beam combining experiment. We achieved efficient combining and demonstrated electronic beam steering of chirped optical waves by tuning the electronic offset oscillator phase in one of the heterodyne OPLLs.

The key physical result driving this work is that swept-frequency optical waveforms suppress stimulated Brillouin scattering (SBS) in fiber by reducing the effective length over which SBS occurs. This has the potential to increase the maximum output of high-power fiber amplifiers; and the chirped phase-locking techniques developed in this thesis can be used to form coherent amplifier arrays, further scaling the optical power. Conventional SBS suppression techniques result in a decrease of the seed laser coherence length, and coherent combining therefore requires very strict path-length matching. In practice, sub-mm matching is necessary at the kW power level. The chirped-seed combining approach developed in this thesis does not have strict matching requirements, due to the comparatively long coherence lengths of SCL-based SFLs, and therefore presents a viable path towards high-power continuous-wave sources.

We have also performed, for the first time, an active CBC experiment using a chirp rate of 5×10^{14} Hz/sec and two 3 W erbium-doped fiber amplifier channels. We recorded a threefold increase of the amplifier SBS threshold, when compared to a single-frequency seed. We demonstrated efficient phase-locking and electronic beam steering of amplified chirped beams, and achieved temporal phase noise levels corresponding to fringe visibilities exceeding 90% at path-length mismatches of $\approx$ 300 mm, and exceeding 98% at a path-length mismatch of 20 mm.

7.2 Current and Future Work

The ground for continuing SFL development is fertile. One of the projects undertaken in our group, led by Yasha Vilenchik, is the integration of the optical components of the optoelectronic SFL on a hybrid Si/III-V integrated platform. Images of the subcomponents fabricated to date are shown in figure 7.1. The hybrid platform has the potential to bring photonic and electronic components together on a single bonded chip, and continuing development will one day yield a chip-scale chirped LIDAR transmitter.

Another interesting development in our group is the recent demonstration of a hybrid Si/III-V high-coherence semiconductor laser based on a modulated-bandgap design, shown in figure 7.2 [106]. The laser's high-Q resonator, designed and fabricated by Christos Santis, is contained entirely in silicon, and is therefore subject to much lower optical loss than traditionally used III-V resonators. This laser's chirp bandwidth is comparable to that of commercially available DFBs, while its linewidth is inherently superior. The use of this laser in an optoelectronic SFL will enable 3-D imaging systems that simultaneously possess long imaging range and high axial resolutions.

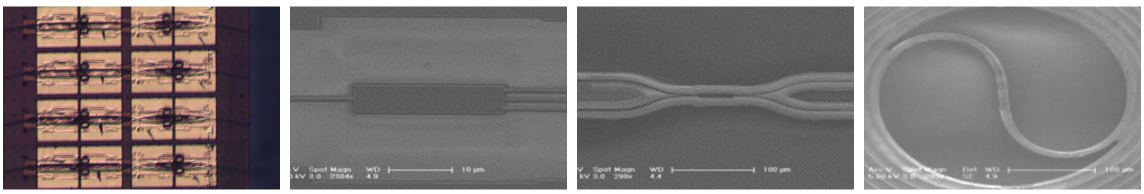

(a) (b) (c) (d)

Figure 7.1: (a) Hybrid Si/III-V DFB laser bar. (b) Scanning electron microscope (SEM) image of a 1×3 multimode interference (MMI) coupler, (c) SEM image of a 2×2 MMI coupler. (d) SEM closeup of the a spiral delay line for the loop MZI

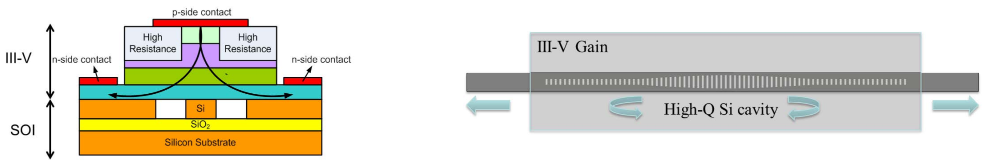

(a) (b)

Figure 7.2: Schematic of the hybrid Si/III-V high-coherence semiconductor laser. (a) Side-view cross section. (b) Top-view of the laser and the modulated-bandgap resonator

Development of narrow-linewidth swept-frequency lasers will also contribute to the group's label-free biomolecular sensing project, led by Jacob Sendowski. The sensor comprises an ultra-high-Q SiN microdisk resonator and a microfluidic analyte delivery system [15], as shown in figure 7.3. Biomolecular binding events shift the microdisk resonance frequency, which is detected using the optoelectronic SFL. Long-term repeatability of the starting frequency of SFL sweeps was a deciding factor in using it to interrogate the biomolecular sensor. The use of narrow-linewidth SFLs has the potential to improve measurement sensitivity by enhancing the sensor's ability to resolve small resonant frequency shifts. Moreover, integration of the SFL will enable a complete chip-scale high-sensitivity biomolecular sensor.

Recent developments in the field of microelectromechanical (MEMS) VCSELs hold promise for SFLs with extremely high chirp rates [107]. These devices are based on an electrically-tunable MEMS mirror, and are capable of sweeping a bandwidth of 100 nm at a wavelength of 1060 nm, with repetition rates exceeding 100 kHz. This corresponds to a chirp rate $> 10^{18}$ Hz/sec, which is two orders of magnitude higher than the fastest SFLs constructed with conventional SCLs.

Our chirped-waveform CBC experiments are currently being repeated at 1060 nm using the VCSEL-based SFL. This is the wavelength of choice for high-power laser sources because of the extremely efficient Yb-doped fiber amplifier technology. The development of an SFL based on the 1060 nm MEMS VCSEL will yield unprecedented chirped-seed SBS suppression results, due to the extremely high chirp rates attainable with these devices.

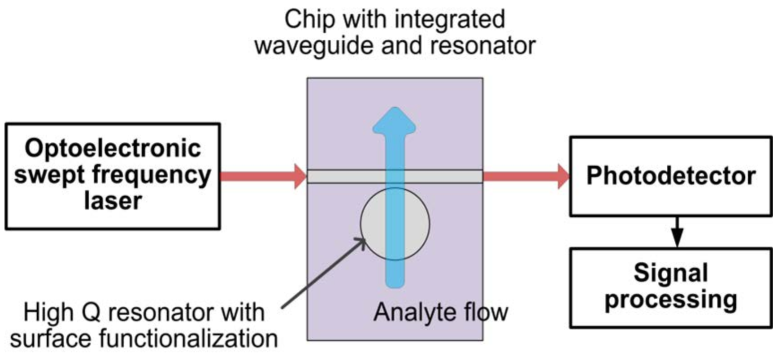

Figure 7.3: Schematic representation of the label-free biomolecular sensing system

TomICam experiments aimed at demonstrating full 3-D imaging capability using a low-cost silicon CCD camera are currently being performed in our group. These experiments rely on our 1060 nm DFB and VCSEL SFLs for illumination. A preferred wavelength for silicon sensors is 850 nm, and we are currently developing an 850 nm VCSEL-based SFL to address this demand. Recently-demonstrated 850 nm MEMS VCSELs [108] can be used to build SFLs that will enable μm-scale axial resolutions in our TomICam systems. An alternative path towards increasing TomICam axial resolution is through the use of MS-FMCW. Hardware stitching can be adopted to the TomICam platform in a very straightforward way, and an array of 850 nm VCSELs can therefore be used for broadband swept-frequency illumination.

In summary, electronic control over the frequency of semiconductor lasers enables a range of swept-frequency applications, from spectroscopy and biomolecular sensing, to ranging and 3-D imaging, to stimulated Brillouin scattering suppression in, and coherent combining of high-power fiber amplifiers. Continuing development and integration of the SFL technology holds promise for chip-scale coherent sensing and 3-D imaging systems.